IEEE Access
Multidisciplinary | Rapid Review | Open Access Journal

Received June 13, 2017, accepted July 5, 2017, date of publication July 13, 2017, date of current version August 8, 2017.

Digital Object Identifier 10.1109/ACCESS.2017.2726017

Supervisory Control for Resilient Chiller Plants Under Condenser Fouling

KHUSHBOO MITTAL[1], JAMES P. WILSON[1], BRIAN P. BAILLIE[2], SHALABH GUPTA[1], (Member, IEEE), GEORGE M. BOLLAS[2], AND PETER B. LUH[1], (Life Fellow, IEEE)

[1]Department of Electrical and Computer Engineering, University of Connecticut, Storrs, CT 06269, USA
[2]Department of Chemical and Biomolecular Engineering, University of Connecticut, Storrs, CT 06269, USA

Corresponding author: Shalabh Gupta (shalabh.gupta@uconn.edu)

This work was supported by the UTC Institute for Advanced Systems Engineering, University of Connecticut. Any opinions expressed herein are those of the authors and do not represent those of the sponsor.

ABSTRACT This paper presents a supervisory control strategy for resilient chiller plants in the presence of condenser fouling. Fouling results in off-nominal performance of chiller parameters, such as increased refrigerant mass flow rate, compressor motor speed, discharge pressure, and discharge temperature. These effects further lead to faster deterioration of condenser pipes and tubes, and increase the risk of early motor failures. Thus, the main objective of this paper is to provide resilience, i.e., to bring the system parameters back to normalcy, and thereby protect the system from the adverse effects of fouling and improve its life expectancy while ensuring energy efficiency and meeting the desired cooling load. The supervisory control strategy presented here incorporates *fault detection and diagnosis* (FDD) and *resilient control* for mitigating the effects of condenser fouling. A computationally efficient and robust FDD scheme enables the estimation of the condenser fouling level using optimal sensor selection and statistical classifiers, thus facilitating condition-based maintenance. On the other hand, the resilient control scheme enables redistribution of load between chillers in order to reduce the load on faulty equipment in an energy-efficient manner, while still providing the required overall cooling load. The performance of this method is tested and validated using a high-fidelity chiller plant model and the proposed strategy is shown to diagnose condenser fouling with a high accuracy and effectively mitigate the effects of fouling at low computational cost. It is shown that the supervisory controller is able to meet the desired building load requirements at lower energy consumption, as compared with no supervisory control.

INDEX TERMS Resilient control, fouling diagnosis, sensor selection, chiller plants.

I. INTRODUCTION

Chiller plants are responsible for providing thermal comfort and acceptable air quality in buildings and account for a significant portion of world's energy consumption [1], [2]. Fig 1 shows a schematic diagram of a chiller plant. A typical chiller plant is a large, complex, and interconnected system that consists of multiple chillers, cooling towers, water pumps, and their associated components (e.g, a chiller consists of a condenser, an evaporator, and a compressor, etc). Chiller plants provide cooling to the buildings by means of efficient vapor-compression refrigeration cycles. Furthermore, chiller plants operate under time-varying cooling loads in response to different weather conditions. Thus, the complexity of a chiller plant makes it susceptible to the growth of faults in its components, such as condenser and evaporator fouling, compressor motor faults, refrigerant charge degradation, sensor faults, etc. These faults gradually evolve over time and lead to equipment degradation and inefficient plant operation resulting in increased energy costs. Moreover, operating with degraded equipment results in decreased component lifetime, thus increasing the equipment maintenance and replacement costs. In severe cases, the inability of the degraded component to meet its performance causes occupant discomfort in buildings.

A. MOTIVATION

This paper focuses on condenser fouling since it is one of the most common faults in chiller plants [3]–[5]. Condenser fouling is caused by accumulation of foreign substances on the inner surface of the condenser, which decreases the effective heat transfer area and increases the thermal resistance. This diminishes the efficiency of heat transfer

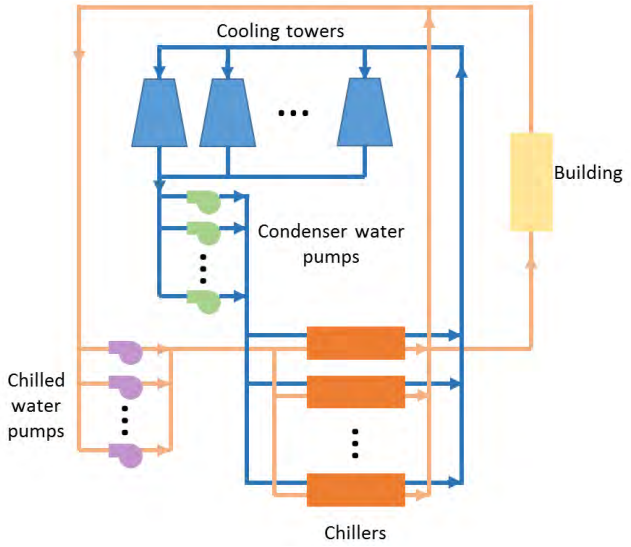

FIGURE 1. Schematic of an interconnected chiller plant.

TABLE 1. Effects of fouling on a chiller system.

Effect on parameters	Degradation, wear and other effects
High discharge pressure	Pipe leakage and bursts, undue load on compressor [8]
High refrigerant flow rate	Low Superheat temperature causing damage to compressor by liquid entry
High discharge temperature	Compressor overheating problems, material degradation and excessive thermal expansion [7]
High compressor speed	Early wear of motor, breakdown of insulation
High compressor power	Inefficient energy consumption, excessive load on compressor motor
High chilled water supply temperature	Desired indoor temperature not maintained, discomfort in buildings
Low cooling load supply	Building load demand is not met, discomfort in buildings

between the two fluids of the condenser leading to chiller inefficiency.

In order to compensate for this deficiency and to meet the required cooling load, the chiller controller increases the refrigerant pressure and mass flow rate through the condenser by raising the compressor speed. This leads to higher power consumption, reduced energy efficiency, and increased wear of the chiller components (e.g., pipes, tubes, motors, etc.). While high refrigerant mass flow rate and high pressure lead to faster deterioration of condenser pipes and tubes, a higher compressor speed increases the risk of early compressor motor failures. In effect, the entire system operates as a stressed congested system trying to meet the demand. Table 1 summarizes the several adverse effects of fouling on chiller health and performance [6]–[8]. Under severe fouling conditions, the degraded chiller might not even be able to meet its demanded cooling load despite overdriving the compressor, resulting in thermal discomfort to building occupants and significantly reducing the long-term reliability of chiller components.

Therefore, this paper develops a supervisory control strategy whose main objective is to provide resilience to the chiller plants by load reconfiguration i.e., redistributing the load of the faulty chiller between the healthy chillers. It brings the system parameters back to normalcy and results in mitigation of the effects of condenser fouling, while maintaining energy efficiency and meeting the desired cooling load performance. The major challenges faced by the the proposed supervisory control framework are summarized in Fig. 2.

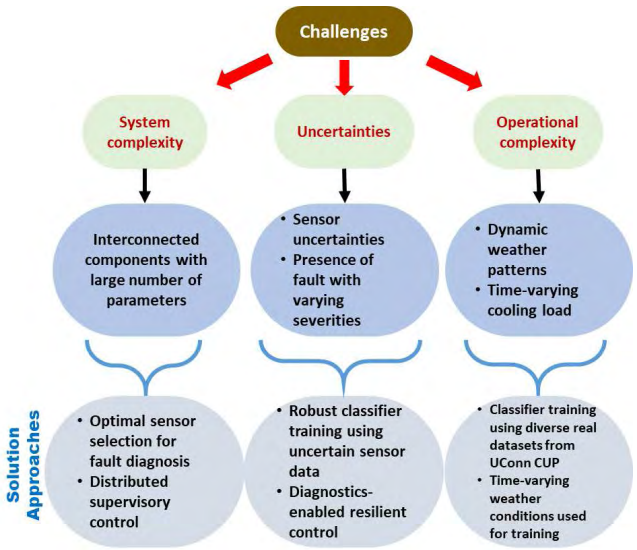

FIGURE 2. Challenges and the proposed solution approaches.

Remark: The objectives of a resilient controller [9]–[12] are far beyond a fault-tolerant controller. A fault-tolerant controller strives to meet the desired performance of an output variable in the presence of faults. In this process, it can possibly drive the system more rigorously thus causing further damage to the already faulty system. On the other hand, a resilient controller strives to bring all the system parameters back to normalcy to improve system reliability, thus mitigating the effects of faults and preventing further damage. This however could be done with a graceful degradation of performance if necessary.

B. LITERATURE REVIEW

Many researchers have developed optimization-based supervisory control strategies with the main focus on improving the energy-efficiency of chiller plants [13]–[18], however these approaches did not consider faulty operating conditions. On the other hand, some researchers have shown interest in developing fault-tolerant control methodologies for variable air volume (VAV) air conditioning systems. For example, Wang and Chen [19] developed an energy efficient fault-tolerant controller that addresses the air flow rate sensor measurement faults using neural networks to estimate measurement errors. Jin and Du [20] designed a fault tolerant

TABLE 2. Literature review of the existing research for fault tolerant control of condenser fouling.

Authors	Objective	Methodology	Research Gaps
Ma et al. [22], [23]	Fault-tolerant control scheme for various condenser cooling water system faults	Model predictive control (MPC) and hybrid quick search (HQS) optimization	Although fault tolerant controllers for energy minimization of chiller plants exist in literature, the resilience aspect of bringing the system parameters back to normalcy for increasing system reliability has not been addressed
Liu et al. [24]	Fault tolerant supervisory control of variable air volume air-conditioning systems in the presence of water-side and air-side fouling	Use of fuzzy models for prediction of control performance, selection of set points minimizing the total power consumption of the plant	

controller for controlling outdoor air and AHU supply air temperature of VAV systems in case of sensor bias faults. The proposed method uses PCA and joint angle method for detection and isolation of fault and compensatory reconstruction for fault reconstruction. Ji et al. [21] developed a prognostics-enabled resilient controller for building climate control systems in order to maintain an accepted level of thermal comfort in the presence of component failures. Specifically, for condenser fouling, Table 2 discusses the existing work in the area of fault-tolerant control to accommodate this fault and also the current research gaps.

One major limitation of the aforementioned approaches is that they used simplified chiller plant models to determine the optimal set points for the plant. The use of simplified models limits the availability of critical variables, such as the compressor speed, thus making it difficult to directly study the system-wide impact of faults. In addition, the fault tolerant controllers are primarily focused on meeting the performance and energy requirements; however they did not touch upon the essence of *resilience*, i.e., to bring the system back to normalcy, in presence of faults. In particular, there has not been significant research on supervisory control to mitigate the effects of condenser fouling, while meeting the necessary trade-offs between energy-efficiency and resilience. This paper addresses this gap by developing a supervisory control strategy, that enables a resilient controller in presence of condenser fouling, thereby redistributing the load between chillers to protect the faulty chiller from the damaging effects of fouling, while at the same time minimizing the power consumption and meeting the overall cooling load demand. The proposed strategy is validated on a physics-based high-fidelity chiller plant model that utilizes the real cooling load and historical weather data with uncertainties as inputs and includes the necessary performance and control variables.

In order for the supervisory controller to be effective, a robust *fault detection and diagnosis* (FDD) approach is necessary to maintain state awareness of the system and to accurately determine the fault severity. Early detection of condenser fouling is challenging since it is a soft fault that develops slowly over time and often goes unnoticed, causing gradual degradation in the performance of the chiller [4]. There are several existing methods in literature for detecting HVAC system faults and an elaborate review of these methods is presented in [25]–[27]. In general, FDD approaches consist primarily of (1) model-based, (2) knowledge-based and (3) data-driven methods. Existing FDD approaches for common HVAC faults including condenser fouling comprise rule-based methods [28], estimation of residue and thresholding methods [29]–[31], and more sophisticated machine learning based methods, such as principal component analysis (PCA) [32], wavelet transforms [33] and neural networks [34].

Most of the existing FDD approaches rely on human expertise to select the sensors for decision making. However, different sensors have different sensitivities towards faults under time-varying operating conditions. Therefore, the selected sensors are not guaranteed to provide the best FDD performance and classification accuracy. This paper also addresses this shortcoming by performing optimal sensor selection to pick the smallest sensor set that gives the highest classification accuracy. Additionally, instead of binary classification of fouling, the proposed FDD strategy classifies it into multiple categories to provide a better estimate of the severity.

C. CONTRIBUTIONS

The main contributions of the proposed supervisory control framework are summarized as follows:

- Development of a supervisory control strategy that enables a resilient controller for the faulty chiller, to bring its parameters back to normalcy, while minimizing power consumption and providing the desired cooling load.
- Identification of the smallest optimal sensor set for fouling detection and diagnosis in order to reduce the computational complexity of the classifier while maintaining high classification accuracy and low false alarm rate.
- Validation on a high fidelity chiller plant model that takes real building cooling load and weather data with uncertainties as inputs for simulation of faults and data generation.

The rest of the paper is organized as follows. Section II formulates the supervisory control problem for chiller condenser fouling. Section III presents the details of the chiller plant simulation model and describes the effects of condenser fouling. Section IV presents the solution methodology that diagnoses and mitigates the effects of condenser fouling in a robust and energy-efficient manner. Section V shows the results achieved by the proposed methodology. Finally, section VI concludes the paper with recommendations for future work.

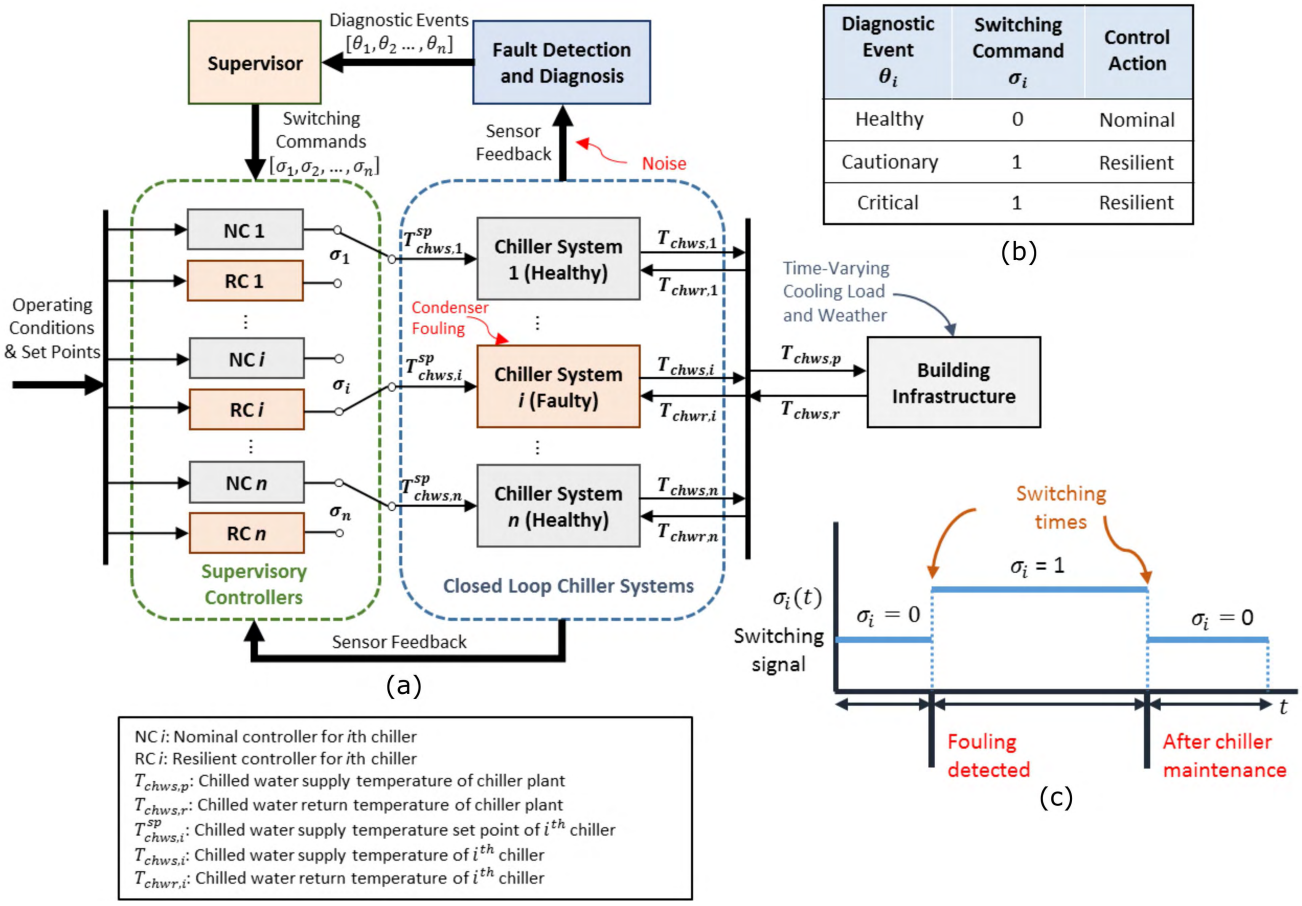

Diagnostic Event θ_i	Switching Command σ_i	Control Action
Healthy	0	Nominal
Cautionary	1	Resilient
Critical	1	Resilient

FIGURE 3. **Proposed supervisory control scheme: (a) supervisory control architecture (b) switching commands and control actions for different diagnostic events (c) illustration of switching for a chiller.**

II. PROBLEM FORMULATION

Traditionally, fouling is treated by periodic maintenance of the chiller plants. However, frequent scheduling for maintenance is expensive and turning off a chiller in summer months is undesirable. Alternatively, if the mean time between successive maintenance routines is large, the growth of condenser fouling can lead to inefficient plant operation. Thus, it is desired to shift from this static time-based maintenance paradigm to a dynamic *condition-based maintenance* (CBM) strategy for achieving cost efficient operation. The goals of the supervisory control are thus clear; in order to overcome the effects of condenser fouling, the proposed strategy must:

- Detect and diagnose condenser fouling to facilitate timely resilient control action to mitigate its adverse effects,
- Provide the desired chilled water supply temperature,
- Reduce the load on the faulty chiller to prevent further degradation of its components due to the effects of fouling, and
- Minimize the chiller plant energy consumption in the presence of condenser fouling.

The following assumptions are made to achieve the desired control action:

- The chiller plant always runs in the safe operating range.
- The plant has redundancy in terms of chillers which are sized such that their maximum cooling load supply is higher than the demand.

A supervisory control architecture designed to meet the above goals is shown in Fig. 3(a). As seen on the right, each chiller is a closed loop system with its own local controller. The supervisory controller consists of a bank of high-level controllers which act on top of these local chiller controllers. Corresponding to each chiller there are two high-level controllers, which are the Nominal Controller (NC) and the Resilient Controller (RC). The nominal controllers for the healthy chillers focus on performance and ensure that the desired overall chilled water supply temperature is met. Simultaneously, the resilient controller for the faulty chiller focuses on resilience by reducing the load on the faulty chiller by reducing its compressor speed. Thus, the load on faulty chiller is automatically redistributed to the healthy chillers to meet the overall cooling demand. This supervisory control action brings the system back to normalcy as much as possible, such that the total energy consumption of the plant decreases. The supervisor performs switching between these two controllers for each chiller based on the feedback

on fault classification from FDD. Thus the supervisor has the mapping $\boldsymbol{\sigma} = \mathrm{S}(\boldsymbol{\theta})$, where $\boldsymbol{\theta} = \{\theta_1, \theta_2, \ldots \theta_n\}$ and $\boldsymbol{\sigma} = \{\sigma_1, \sigma_2, \ldots \sigma_n\}$ are the vectors that correspond to the diagnostic events and the switching commands for all n chillers, respectively. Here, each $\theta_i \in \boldsymbol{\theta}$ carries a decision from the diagnostic decision set {Healthy, Cautionary, Critical}. Also, each $\sigma_i \in \boldsymbol{\sigma}$ carries a command from the command set {0, 1}, where 0 corresponds to NC and 1 corresponds to RC. The mapping is based on a simple logic as shown in the table in Fig. 3(b). Fig. 3(c) illustrates the switching command of the supervisor for the ith chiller based on the FDD feedback. When fouling is detected, the chiller control is switched to RC and after a maintenance action, the supervisor switches it back to NC. The switching can happen at most once in every 12 hour interval after the arrival of diagnostic decision. Details are in Section IV-B.

The FDD methodology classifies fouling into one of the three classes with different fouling severities defined as:

- Healthy (H): Fouling severity $< 20\%$
- Cautionary (Ca): $20\% \leq$ Fouling severity $< 60\%$
- Critical (Cr): Fouling severity $\geq 60\%$.

The critical class, as the name suggests, refers to instances of very high fouling, which results in serious performance degradation and large energy losses. The cautionary class refers to a more frequent minor blockage which often goes unnoticed because the local controllers overdrive the chillers to meet the cooling load demand. In general, the number of classes can be set according to the user requirement. In this work, three classes are chosen as they are able to capture the different fouling severities successfully and the control gains do not vary significantly between the two faulty classes. The chillers in cautionary and critical conditions need a resilient control action as although the cooling load demand might be met in these cases, but the system parameters still perform off-nominally. Aside from minimizing the false alarm and missed detection rates, the FDD approach must:

- Be robust to uncertainties,
- Account for time-varying operating conditions,
- Utilize a minimal amount of sensor data, and
- Perform on low-cost computational platforms.

These requirements are met by using simple but efficient machine learning approaches including a combination of optimal sensor selection techniques, and computationally efficient statistical classifiers. Lastly, a high-fidelity chiller plant model is used for this study as the platform for validating the supervisory control methodology. This simulation model has three centrifugal chillers and takes in real data as its inputs, namely, the time-varying building cooling load, and the weather data, as described in the next section.

III. HIGH FIDELITY CHILLER PLANT MODEL

Simulation models of chillers and other HVAC system components have long been used as tools for making informed plant design decisions and for the development of optimal control strategies [35]–[37]. The models most commonly used in these efforts are highly abstracted and represent chiller performance through relatively simple empirical correlations [38]–[40]. The level of abstraction of these models is such that the entire refrigerant side of chiller, including the compressor, is fully abstracted and replaced with simplified performance curves. These models are useful for describing system behavior at nominal conditions but lack the fidelity necessary for the representation of faults or other system states beyond nominal operation and for the assessment of operating conditions within the chillers. Therefore, the development of a resilient supervisory controller requires a more detailed model.

The models used in this work are developed in Modelica [41] using component models from the Modelon ThermalPower, VaporCycle, and ThermoFluid commercial libraries as well as the Modelica Buildings Library and the ThermoCycle open source library [42]–[44]. The chiller plant model integrates submodels representing each of the major components of the chiller plant. Models for the pumps, pipes, cooling towers, and building-side heat exchangers are included. A number of assumptions are made regarding the operation of the plant. Water flow rates for both the chilled and cooling water loops are kept constant and all components of the plant are always active rather than staging to match load conditions.

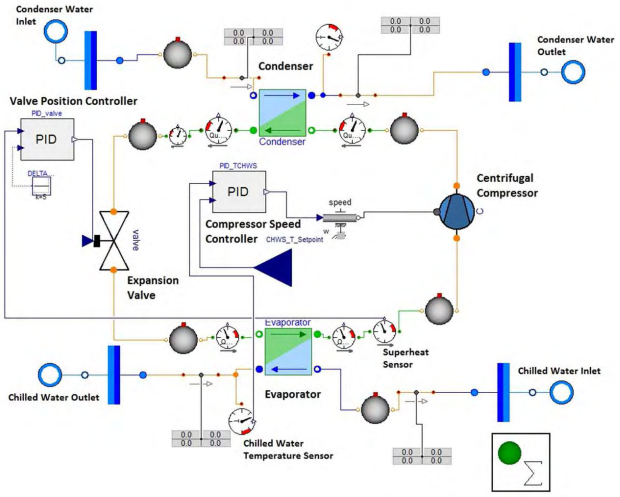

FIGURE 4. Modelon-library based centrifugal chiller model.

The centrifugal chiller model used here includes component models representing the compressor, condenser, expansion device, and evaporator of a typical vapor-compression chiller, as shown in Fig. 4. The condenser and evaporator are counter-flow heat exchangers with a finite-volume formulation. This formulation divides the heat exchanger into a number of subunits along its length and considers temperatures, heat transfer rates, and fluid properties separately for each subunit. The compressor and expansion devices are represented by static models, with compressor performance defined by a centrifugal compressor characteristic map and valve behavior defined by a direct linear relationship between

mass flow, pressure drop, and opening position. A two-phase fluid media model for R134a refrigerant from the Modelon library [45] is used to determine fluid properties within the chiller subcomponents. These detailed component and fluid property models provide additional information and insight as to the conditions within the chiller over the range of operation as compared to the simplified empirical models frequently used in other work.

The control scheme in the chiller model uses a pair of decoupled PI controllers. The opening position of the expansion valve is manipulated to maintain refrigerant superheat at the compressor inlet, and the operating speed of the compressor is manipulated to maintain the chilled water supply temperature set point. These controllers cannot be modified by the supervisory controller, however their setpoints could be adjusted.

System performance at nominal or faulty conditions can be predicted over a wide range of operating states through dynamic simulation. Historical weather [46] and corresponding cooling load data from the University of Connecticut Central Utilities Plant (UConn CUP) are used as inputs to the model for simulation of a large set of realistic conditions. The chiller plant model was validated through comparison of the simulation results to those of existing validated models and to additional operating data from the UConn CUP. These comparison results are summarized in the Appendix, thus validating that the outputs generated by the simulated model closely follow the trend of the real plant outputs. Further details on the model, plant data, and the simulations executed for verification of model accuracy and significance are presented in [47].

A. MODELING CONDENSER FOULING

For each pair of finite volumes considered in the condenser, the flow of energy from the refrigerant to the cooling water is defined by the simple heat transfer equation as follows:

$$\frac{dQ}{dt} = UA\Delta T \tag{1}$$

where the rate of heat transferred over time is the product of the temperature difference between the two fluids (ΔT), the contact surface area (A), and the overall heat transfer coefficient (U). The primary observed effect of condenser fouling is a reduction in the rate of heat transfer. Water-side fouling of the condenser is injected in the model by adding a fouling coefficient to the right hand side of Eq. 1 equal to one minus the percentage of fouling, representing a decrease in heat transfer coefficient and effective area of the water pipes, thus changing the combined UA value to reduce heat transfer effectiveness in a manner equivalent to that used in Zhao et al. [48]. This increased heat transfer resistance creates a need for either higher temperature or mass flow rate on refrigerant side in order to provide the same cooling. This requires the controller to run the compressor at a higher speed, thus drawing more power and accelerating wear and tear.

TABLE 3. Typical sensors available in a chiller plant.

System	Parameters	Sensors
Chiller	Mass flow rate	Chilled Water Mass Flow Rate
		Condenser Water Mass Flow Rate
	Temperature	Inlet Condenser Water Temp.
		Outlet Condenser Water Temp.
		Discharge Temperature
		Chilled Water Supply Temp.
		Chilled Water Return Temp.
	Pressure	Inlet Condenser Water Pressure
		Outlet Condenser Water Pressure
		Discharge Pressure
		Outlet Condenser Refrigerant Pressure
	Speed	Chiller Compressor Speed
	Power	Chiller Compressor Power
	Performance Metric	Chiller COP*
	Cooling Load	Chiller Cooling Load Supplied*
Chiller Plant	Temperature	Chilled Water Supply Temp.
		Chilled Water Return Temp.
		Ambient Temperature
		Wet-Bulb Temperature*
	Power	Total Power of all Chillers*
	Cooling Load	Total Building Cooling Load Supplied*

*Not actual physical sensors, but derived from other sensors.

B. FAULT DATA GENERATION USING REAL COOLING LOAD AND HISTORICAL WEATHER DATA AS MODEL INPUTS

The high fidelity chiller plant model described above is used for generating data for classifier training for fault diagnosis. In order to simulate realistic and uncertain plant operating conditions, cooling load data for the months of June, July and August from the years 2013 and 2014 were taken from UConn CUP and given as inputs to the plant model. Historical weather data [46] including ambient temperature, relative humidity, and sea level pressure for the same days were also used as model inputs to calculate the wet-bulb temperature [43]. The variations in these input parameters for the first five days of July 2013 are shown in Fig. 5. Furthermore, in order to account for sensor uncertainties, 30 dB of additive white Gaussian noise (AWGN) is added to the sensor data as suggested by our industry partner.

Sensor data are collected by simulating the model under these operating conditions at a sampling rate of $\frac{1}{60}$ Hz which is in accordance with the limitations discussed with our industry partner. Table 3 lists the most important sensors available in the plant. For brevity, the variables derived from measured values are also referred to as 'sensors', such as the chiller coefficient of performance (COP). COP is used to report the efficiency of refrigerant based systems. It is the ratio of the amount of cooling supplied by the evaporator compared to the energy consumed by the compressor.

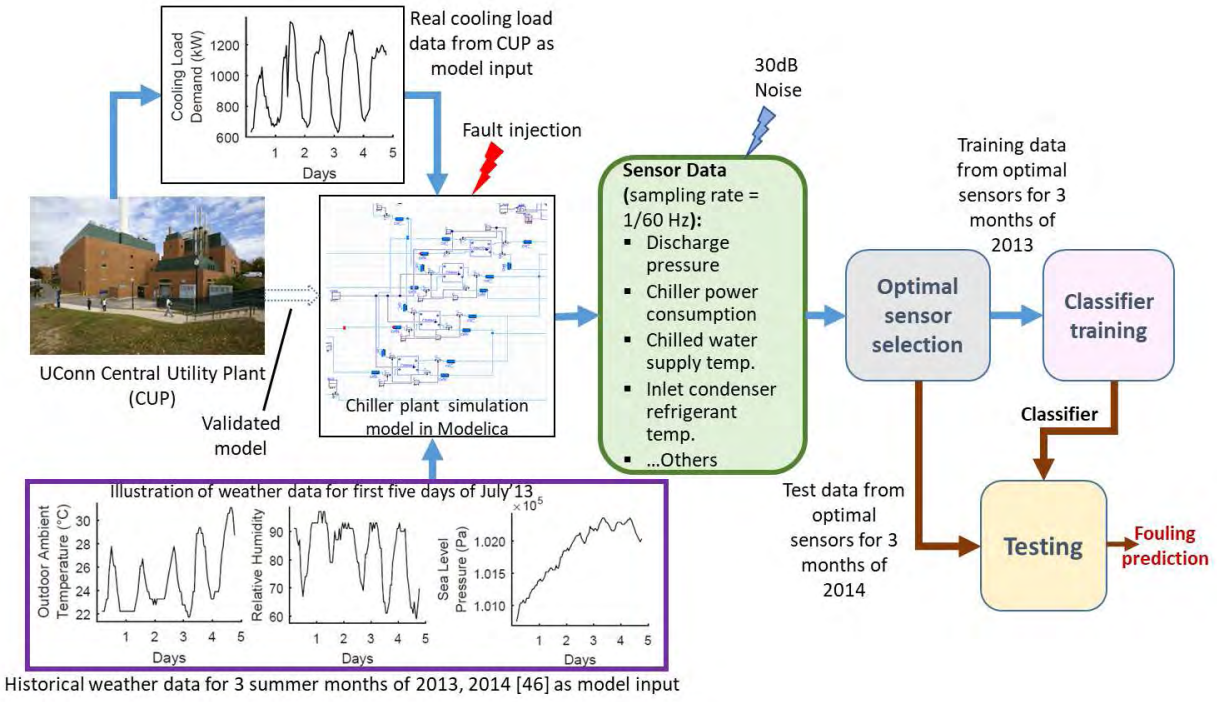

FIGURE 5. FDD structure that utilizes sensor data generated from a high-fidelity chiller plant model using inputs of i) real cooling load data from UConn CUP and ii) historical weather data, for optimal sensor selection and classifier training.

Condenser fouling is simulated in the model as described in the previous section, where the percent decrease in heat transfer coefficient and the surface area is approximated as the fouling severity. The sensor data are generated for a total 17 different fouling severity levels which range from 0 to 80% in steps of 5%. Fig. 6 shows the effects of condenser fouling on different sensors during the first five days of July'13. Fig. 6(a) shows the variation of wet bulb temperature during this duration. The most direct impact of fouling is a reduction in the heat transfer efficiency of the condenser. In order to make up for this reduced efficiency, the controller pushes a higher mass flow rate of the refrigerant (Fig. 6(b)). To achieve this high mass flow rate, the compressor must operate at an increased speed (Fig. 6(c)). The speed increases dramatically as degradation becomes more severe and ultimately saturates. The rise in compressor speed causes an increase in chiller power consumption (Fig. 6(d), 6(e)) by several percent and a decrease in chiller COP (Fig. 6(f)). The increased work done by the compressor leads to heat buildup in the condenser, raising temperature of the refrigerant entering and leaving the condenser (Fig. 6(g), 6(h)). Above 60% fouling severity, the compressor speed saturates, when the heavily fouled chiller cannot transfer any more heat through the condenser to meet the water temperature set point, which is fixed at 6.5 °C for each chiller (Fig. 6(i)). As such, the cooling load demand is not met (Fig. 6(j)), indicating severe degradation in chiller performance. Fig. 6(e) shows lower power consumption of the faulty chiller in this case because of the reduced heat transfer in the refrigerant states in the chiller. In addition to accelerated compressor wear, the heat buildup in the condenser shifts the operating refrigerant states on the phase diagram, and the resulting change in pressures (discharge and suction pressure, Fig. 6(k) and 6(l), respectively) significantly changes the operating point on the compressor map.

IV. SUPERVISORY CONTROL DESIGN

The supervisory control architecture shown earlier in Fig. 3(a) maintains state awareness by employing an FDD scheme to detect condenser fouling. Based on the FDD results, a resilient control strategy is employed to bring the faulty chiller parameters back to near-normal and enable smooth operation while minimizing energy consumption.

A. FAULT DETECTION AND DIAGNOSIS

Effective implementation of the supervisory controller requires an accurate FDD method for the correct classification of the health of the system. This paper uses an integrated model-based and data-driven approach which utilizes a physics-based model to generate sensor data and a statistical classifier to perform fault classification. While rule-based and thresholding FDD methods are simple to implement, they are not scalable and tend to perform poorly in the presence of uncertainty. Alternatively, neural networks give good diagnosis but at the expense of significant parameter tuning and computational complexity. Therefore, the k-Nearest Neighbor (k-NN) classifier [49] is chosen in this paper to perform fault diagnosis due to its simplicity, computational efficiency, and high classification accuracy. A k-NN classifier classifies

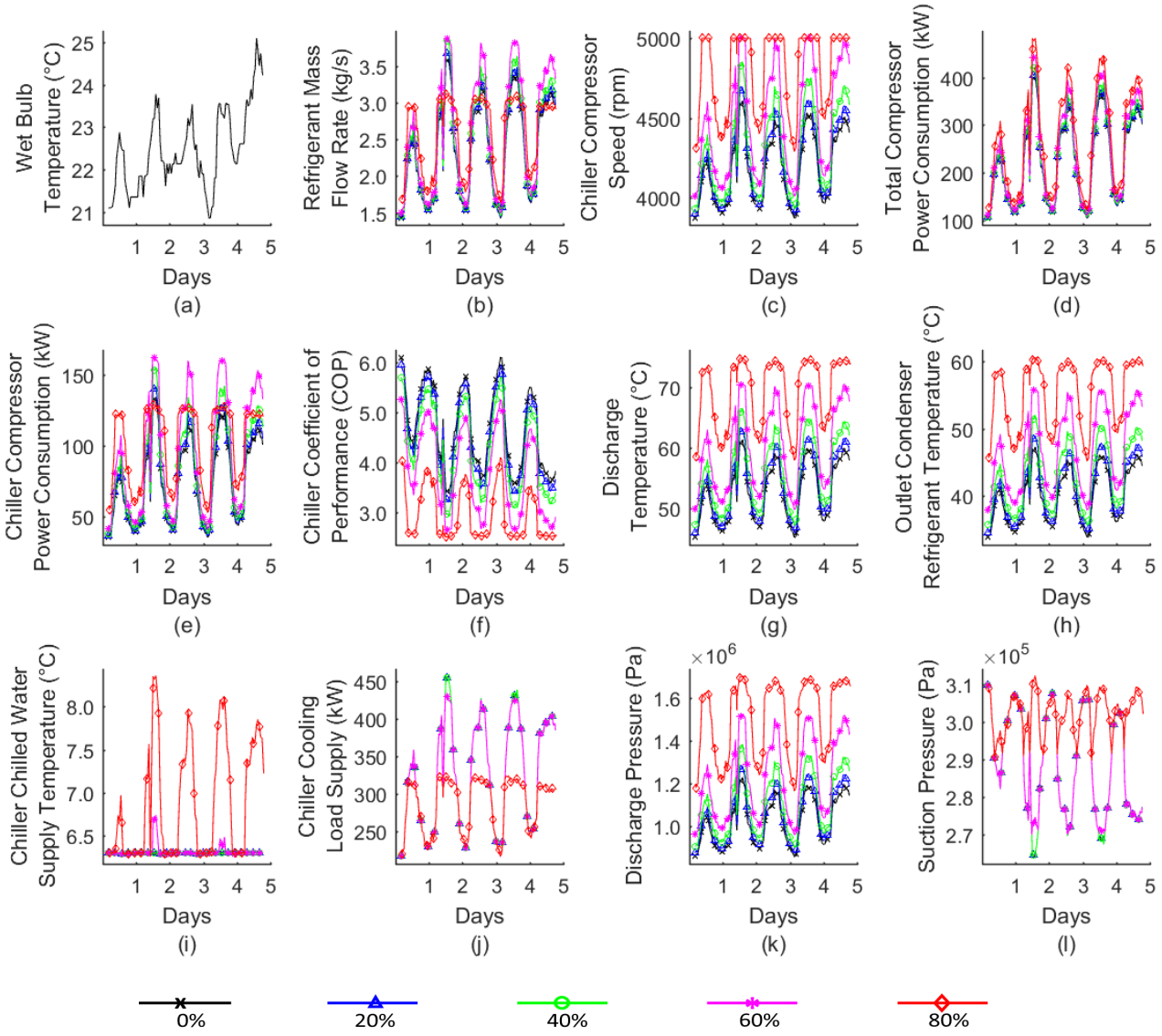

FIGURE 6. Effects of condenser fouling on different sensors (including physically available sensors and the derived ones). Sensor data is shown for the first five days of July 2013.

test data based on the majority vote of its neighbors by assigning the test data to the most common class label among its k nearest neighbors. The training phase of k-NN classifier includes storing all the training data points and their corresponding class labels. The testing phase involves computing the distance between the test data and all the training points to determine the nearest neighbors of the test data and assigning it to the majority class label of the computed neighbors.

Fig. 5 shows the overall FDD architecture. The diagnosis process is comprised of two different phases: (a) training of the classifier for accurate classification of fouling and (b) testing of the trained classifier for performance evaluation.

1) TRAINING

As shown in Fig. 5, the training phase consists of model simulations for data generation, data pre-processing for noise removal, selection of optimal sensors and developing a classification model using the optimal sensors. A detailed description of these steps is presented below.

Sensor data for the months of June, July and August'13 are generated for different fouling severities using the process described in Section III-B. The noisy sensor data is pre-processed by first partitioning the data into blocks of length 720, where each block corresponds to a time duration of 12 hours based on a sampling rate of $\frac{1}{60}$Hz. The data blocks are de-noised by passing through a standard wavelet-based filter [50], [51] and rejecting the end points of the de-noised block by keeping only the mid region of 360 points. The proposed classifier provides a decision for each data point of the de-noised block and the majority vote over all these points is taken as the block decision.

a: SENSOR SELECTION

The filtered data as described above is generated for the different sensors shown in Table 3. To get the best classification accuracy with reduced complexity, optimal sensor selection is important. Several methods exist in the literature for performing optimal sensors selection. Kohavi and John [52] proposed the wrapper method, which is a performance based incremental sensor selection technique, that iteratively adds the sensor that gives the best classification performance to the optimal sensor set. The performance metric used in the wrapper method is the *correct classification rate* (CCR) of the classifier. It is a classifier-based sensor selection approach that becomes computationally expensive if the number of available sensors is large (of the order of 100 sensors). For sensor data sets with a large number of sensors, filter methods (e.g., maximum Relevance Minimum Redundancy (mRMR) [53]) can be used. These approaches first filter the sensor data set to get a smaller sensor subset by using the mutual information between the sensors and the target classes. The wrapper technique is then applied on this filtered sensor subset to get the final optimal sensor data set. Applying a filter method along with the wrapper causes significant reduction in computational complexity for large data sets as only a small subset of sensors is used with the wrapper selection method. In this work, because the number of sensors is small, the wrapper technique is directly applied to the sensor data set to get the optimal sensors.

The steps involved are listed below:

- Initially, set the optimal sensor set as empty, $S^* = \emptyset$, and the available sensor set as S. Sensor data for the months June-Aug'13 is given as input.
- While the total number of optimal sensors is less than N ($N = 4$ here):
  - i) Get a reduced sensor set $\bar{S} = S - S^*$.
  - ii) Evaluate the performance of each sensor subset obtained by adding one sensor at a time from $\bar{S}$ to S^*. The feature space of the k-NN classifier consists of the obtained sensor subset along with the wet bulb temperature (T_{wb}). This is done because even though the sensors have high sensitivity towards fouling severity, they do not have information about the operating conditions. As can be seen in Fig. 6(b), the change in compressor speed for different fouling levels is relative with respect to the magnitude of speed, which is governed by the operating conditions. Thus, in order to add information about the operating conditions, T_{wb} is appended to the feature space comprising the sensor subset. The performance of each feature space is evaluated by using 10-fold cross validation [54] with the k-NN classifier. Various performance metrics like correct classification rate (CCR) and false alarm rate (FAR) can be used. In this paper, CCR is used to rank the sensor subsets. The confusion matrix used for computing these metrics is shown in Table 4. These metrics are defined in Eqs. (2) and (3), respectively.

TABLE 4. Confusion matrix where c_{ij} represents the number of data points belonging to class i and classified as class j.

		Classifier Output		
		Healthy	*Cautionary*	*Critical*
Actual Classes	*Healthy*	c_{11}	c_{12}	c_{13}
	Cautionary	c_{21}	c_{22}	c_{23}
	Critical	c_{31}	c_{32}	c_{33}

$$CCR = \frac{\Sigma_i c_{ii}}{\Sigma_i \Sigma_i c_{ij}} * 100\% \tag{2}$$

$$FAR = \frac{\sum_{j=2}^{3} c_{1j}}{\Sigma_{j=1}^{3} c_{1j}} * 100\% \tag{3}$$

  - iii) Set the optimal sensor set S^* as the subset with the highest CCR.

The optimal sensors selected by using the incremental wrapper selection method are ranked as follows:

1) *Discharge Temperature*
2) *Power Consumption of all Chillers*
3) *Power Consumption of Faulty Chiller*
4) *Chilled Water Supply Temperature*

Initially, the top four optimal sensors are selected, but the number of optimal sensors is a tuning parameter, selected based on classifier performance. To select the best feature space, four different classifiers are trained using different feature spaces. The feature space for the first classifier consists of T_{wb} and the top optimal sensor. Similarly, the feature spaces of second, third and fourth classifiers consist of the top two, top three and top four optimal sensors, respectively, along with T_{wb}. Thus, four different k-NN classifiers are trained to classify the chiller state as healthy, cautionary or critical.

2) TESTING

After training the classifiers with the summer months of the year 2013, their performance is tested on the months of June, July and August of year 2014. Input data from these months is used for model simulations and data generation for known fouling severities. The noisy data set is pre-processed by partitioning the data into blocks of length 720 and de-noising each block. The data from the optimal sensors are then given as input to the trained classifiers. The predicted fouling classes are compared with the original classes and the classification results are presented in Section V-A.

B. SUPERVISORY CONTROLLER

During the nominal operation of chiller plant without implementing the supervisory control, each of the n chillers receive the same set point $T^d_{chws,p}$ for the desired chilled water supply temperature. As shown on the right side of Fig. 7, each chiller has a closed loop controller that regulates the water temperature locally by selecting an appropriate compressor

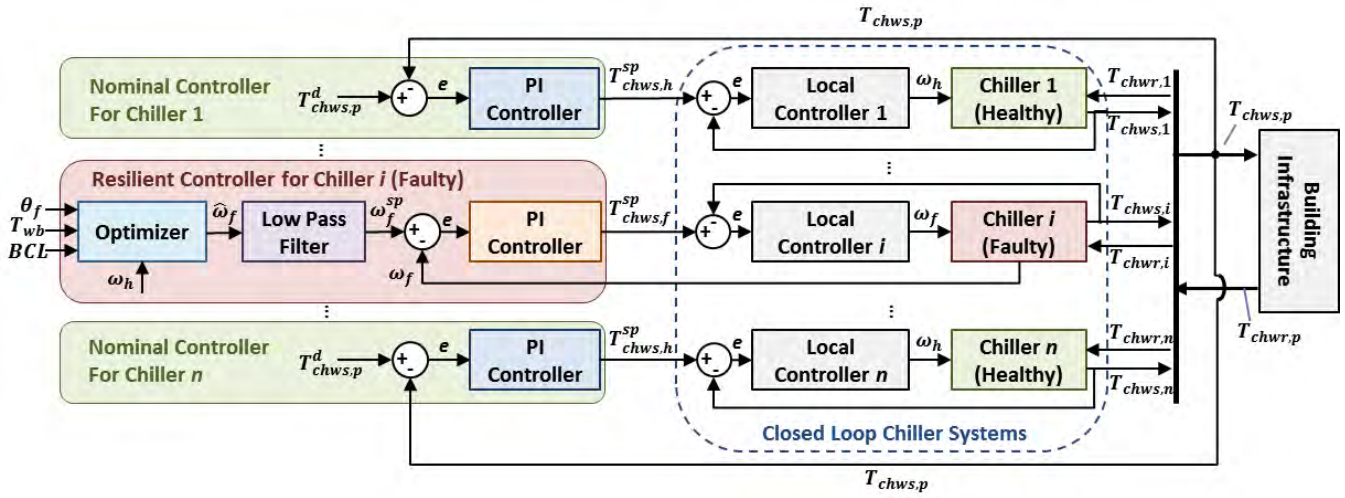

FIGURE 7. Supervisory controllers acting on the healthy and faulty closed-loop chiller systems.

speed $\omega_j(t)$, $j = 1 \ldots n$. The chilled water leaving from the j^{th} chiller with temperature $T_{chws,j}(t)$ mixes with the chilled water from other chillers, thus resulting in the average chilled water supply temperature $T_{chws,p}(t)$, which is then used to cool the buildings. When all chillers are healthy, the desired cooling load is met, such that

$$T_{chws,j}(t) = T_{chws,p}(t) = T^d_{chws,p} \tag{4}$$

Now suppose that there is fouling in the condenser of the i^{th} chiller, then the amount of heat transfer from this faulty chiller reduces. In order to overcome this deficiency, the local controller of this faulty chiller increases the compressor speed in order to increase the mass flow rate and pressure of the refrigerant at the condenser inlet. However, this leads to increased power consumption and increased stress not only on the compressor but also on the other components of the chiller, hence causing accelerated wear. Thus, under these conditions, although the desired cooling load might be met, i.e. $T_{chws,i} = T^d_{chws,p}$, the chiller parameters such as refrigerant mass flow rate, compressor motor speed, discharge pressure, and discharge temperature go off-nominal which is undesirable. Furthermore, in critical cases, that is under severe levels of fouling, the compressor speed saturates, resulting in the inability of the faulty chiller to even maintain the cooling load. As such, $T_{chws,i} > T^d_{chws,p}$, which in turn results in the chiller plant not meeting the desired cooling load, i.e. $T_{chws,p} > T^d_{chws,p}$. In these critical cases, since there is no feedback that monitors $T_{chws,p}$, even the controllers of the healthy chillers cannot take any corrective actions to meet the desired chilled water supply temperature $T^d_{chws,p}$.

Fig. 7 shows the details of supervisory controller which consists of two high-level controllers, the Nominal Controller (NC) and the Resilient Controller (RC) for each chiller. As shown in Fig. 3 earlier, the supervisor switches the control of the faulty chiller from the nominal mode to the resilient mode in presence of condenser fouling. Hence these high-level controllers, i.e. RC on the faulty chiller and NC's on the healthy chillers, operate together such that the load on the faulty chiller is redistributed to the healthy chillers, albeit in an energy-efficient manner. The NC's acting on the healthy chillers focus on performance and ensure that the desired chilled water supply temperature of the plant is met; however, these NC's alone do not make the system resilient to the effects of condenser fouling. In contrast, the RC acting on the faulty chiller focuses on resilience, i.e. bringing the faulty chiller parameters back to normalcy, to prevent accelerated wear of its components. Table 5 lists some useful variables.

As discussed earlier, an immediate effect of fouling is an increase in the compressor speed of the faulty chiller, due to the action of its local controller to maintain the cooling load requirement. Thus it is desired to reduce the compressor speed of the faulty chiller and increase it for the healthy chillers such that the desired temperature $T^d_{chws,p}$ is met, while energy is minimized. However, as per the requirements of our industry partner, the supervisory controller cannot bypass the local controllers, thus the chiller compressor speeds $\omega_j(t)$, $j = 1, \ldots n$, cannot be directly changed. Therefore, $\omega_j(t)'s$ are controlled indirectly by adjusting the set points of individual chillers, i.e. $T^{sp}_{chws,j}(t)$, $\forall j = 1, \ldots n$. Since the overall energy consumption has a nonlinear profile with respect to the compressor speeds, the faulty chiller speed could only be reduced until it hits the minimum energy point. This optimization problem is described in Section IV-B2.

Notation: In the remaining paper, the subscript f is used to denote the index of the faulty chiller, and the subscript h, $h \neq f$, is used to denote the indices of the healthy chillers.

1) NOMINAL CONTROLLERS FOR THE HEALTHY CHILLERS

The objective of this controller is to maintain

$$T_{chws,p}(t) = T^d_{chws,p} \tag{5}$$

TABLE 5. Variables used by the supervisory controller during runtime.

Input Variables to Supervisory Controller		Feedback Variables to Supervisory Controller		Decision Variables		Indirectly Controlled Variables	
$T^{d}_{chws,p}$	Desired chilled water supply temperature of chiller plant (°C).	$T_{chws,p}$	Chilled water supply temperature of chiller plant (°C).	$T^{sp}_{chws,h}$	Chilled water supply temperature set point of healthy chillers (°C).	ω_h	Compressor speed of healthy chillers (RPM)
T_{wb}	Wet bulb temperature (°C).	ω_h	Compressor speed of healthy chillers (RPM).	$T^{sp}_{chws,f}$	Chilled water supply temperature set point of faulty chiller (°C).	ω_f	Compressor speed of faulty chillers (RPM)
BCL	Building cooling load (kW).	ω_f	Compressor speed of faulty chiller (RPM).				
θ	Fouling level (nominal, cautionary, critical).						

by adjusting the set points $T^{sp}_{chws,h}(t)$ of the healthy chillers via monitoring $T_{chws,p}(t)$ as feedback signal, as shown in Fig. 7. Since in this paper all chillers are assumed to have the same cooling capacity and power consumption, all healthy chillers receive the same set point $T^{sp}_{chws,h}(t)$. This controller is implemented as a Proportional-Integral (PI) controller with the following transfer function

$$G_h(s) = K_h\left(1 + \frac{1}{T_h\, s}\right) \tag{6}$$

where $K_h = 0.792$ and $T_h = 6.64$ seconds are the proportional gain and integral time, respectively. The controller was tuned using the Zeigler-Nichols method and was tested to maintain performance under time-varying operating conditions, such as the building cooling load $BCL(t)$ and the wet-bulb temperature $T_{wb}(t)$.

2) RESILIENT CONTROLLER FOR THE FAULTY CHILLER

The NC's running on the healthy chillers always ensure that the cooling load requirement is met, thus any reduction in the cooling provided by the faulty chiller will be compensated by the healthy chillers automatically. Since the faulty chiller is less efficient and more prone to wear than the healthy chillers, it should not work as hard as the healthy chillers and hence $\omega_f(t)$ should be reduced to below $\omega_h(t)$. However, the power profile is nonlinear with respect to compressor speeds and thus $\omega_f(t)$ cannot be arbitrarily reduced. Let $p_j(t)$ be the power consumption of the j^{th} chiller. Then the total power consumption of all chillers is defined as $P_{total}(t) = \sum_{j=1}^{n} p_j(t)$. The RC acting on the faulty chiller reduces $\omega_f(t)$ until the optimal point $\omega^*_f(t)$ is reached where $P_{total}(t)$ is minimum, thereby maximizing the energy efficiency of the system. Thus, the optimization problem is defined as follows:

$$\begin{aligned} &\underset{\omega_f(t)}{\text{minimize}}\ P_{total}(t) \\ &\text{subject to } \omega_f(t) \le \omega_h(t) \end{aligned} \tag{7}$$

Corresponding to $\omega^*_f(t)$, the speed of the healthy chillers, which meets the cooling load demand (i.e. $T_{chws,p}(t) = T^{d}_{chws,p}$), is termed as $\omega^*_h(t)$. Determining $\omega^*_f(t)$ in real time, however, is challenging since it depends on the time-varying input operating conditions such as the building cooling load $BCL(t)$ and the wet-bulb temperature $T_{wb}(t)$, and also the fouling level $\theta_f(t)$ of the faulty chiller.

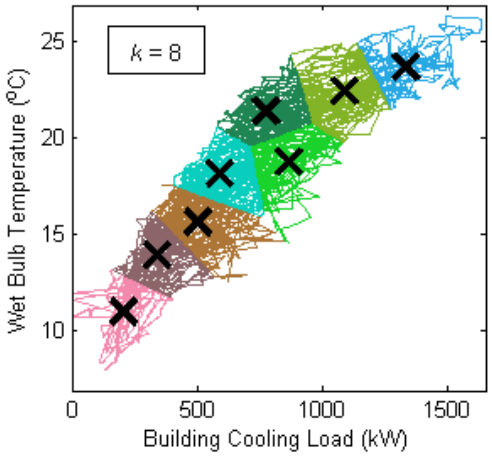

FIGURE 8. *k*-means clustering of the operating space.

a: OFFLINE TRAINING

Since it is difficult to calculate all values of ω^*_f for each operating condition, only a finite number of operating points are considered. These pre-computed values of ω^*_f are later used during runtime to approximate the optimal set points for the chiller plant. In order to select these operating points, the input operating space (BCL, T_{wb}), consisting of the historical cooling load and the weather data, is partitioned into different regions using the k-means clustering algorithm [55]. The results with $k = 8$ for the data from the summer of 2013 are shown in Fig. 8. Then for each centroid and given fouling level of the faulty chiller, the simulation model is run for different values of ω_f with the nominal controller for healthy chillers running. Since the faulty class is either cautionary ($20\% \le$ fouling severity $< 60\%$) or critical ($60\% \le$ fouling severity), the middle points of 40% and 70%, respectively, are chosen as the inputs for each class. Then the outputs of simulation runs are used to generate the power consumption profiles for various input conditions.

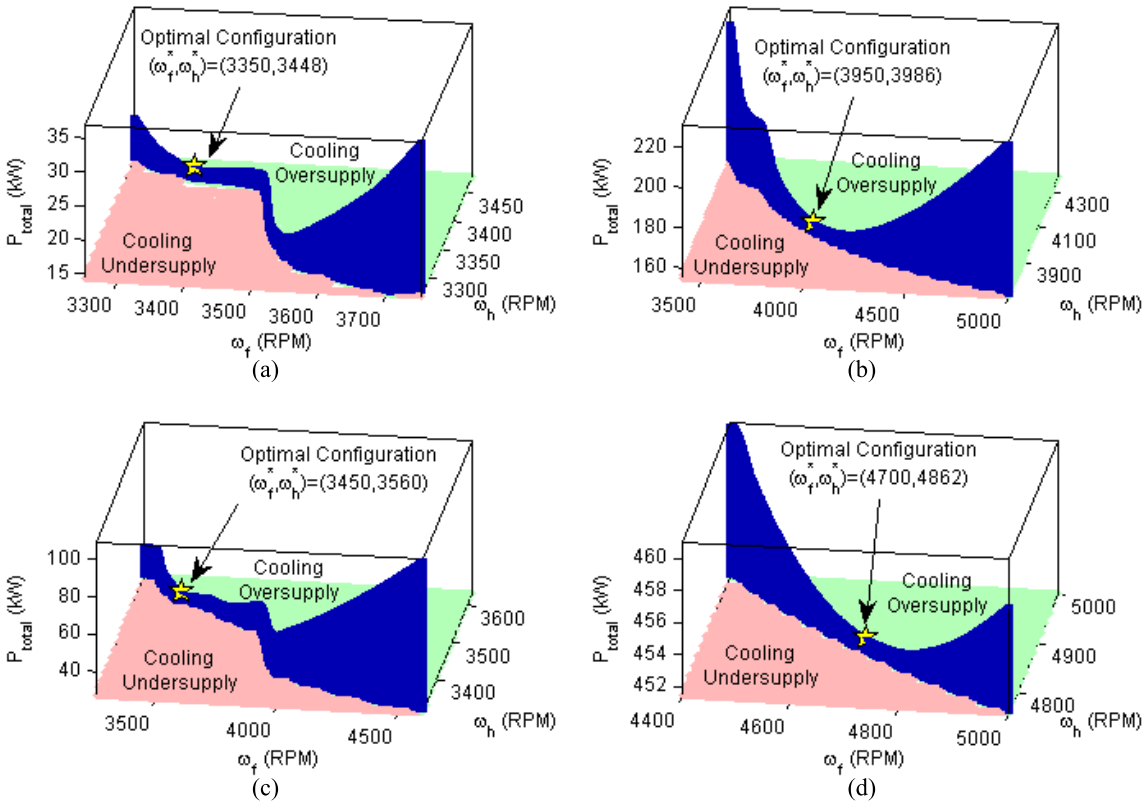

FIGURE 9. Power profiles for four different fouling levels (*FL*), building cooling loads (*BCL*), and wet bulb temperatures (T_{wb}): (a) *FL* = 40%, *BCL* = 207.3 kW, T_{wb} = 11.0 °C (b) *FL* = 40%, *BCL* = 865.3 kW, T_{wb} = 18.8 °C (c) *FL* = 70%, *BCL* = 504.7 kW, T_{wb} = 15.6 °C (d) *FL* = 70%, *BCL* = 1331.6 kW, T_{wb} = 23.7 °C.

These profiles show the relationship between P_{total}, ω_f and ω_h. Four example power profiles are shown in Fig. 9 for four different conditions. P_{total} is only plotted when the required cooling load is met (e.g. $T_{chws,p} = T^d_{chws,p}$). There is an oversupply of cooling in the green region above the P_{total} curve (i.e., $T_{chws,p} < T^d_{chws,p}$), and an undersupply of cooling in the red region below the P_{total} curve (i.e., $T_{chws,p} > T^d_{chws,p}$). These plots also illustrate the nonlinear behavior of the chiller systems. Since there are two fouling classes besides nominal and eight operating condition as determined from the centroids of the clustering, a total of 16 power profiles are constructed. Then, the values of ω_f and ω_h that minimize P_{total} while supplying the required cooling load are selected as the optimal chiller compressor speeds ω^*_f and ω^*_h for each condition. This selection is thus the most energy efficient setting for the chiller plant that still satisfies the operational constraints in the presence of faults.

Additionally, the reduction of $\omega_f(t)$ to $\omega^*_f(t)$ not only reduces the power consumption but also reduces the mass flow rate of the refrigerant in the chiller. This, in turn, reduces the temperature of pressure inside the chiller and therefore reduces the overall stress, thereby mitigating the effects of condenser fouling until proper maintenance can be performed.

b: RUNTIME

During runtime, the optimizer, as shown in Fig. 7, takes the current $BCL(t)$ and $T_{wb}(t)$ and finds the nearest centroid used during offline training. This centroid and the health state $\theta_f(t)$ provided by the FDD, are then used to select the corresponding $\omega^*_f(t)$. This compressor speed, however, is only optimal for the centroid point, and hence it is slightly sub-optimal for the actual operating point. Therefore, the estimate of near-optimal faulty chiller compressor speed $\hat{\omega}_f(t)$, is obtained by the following approximation:

$$\frac{\hat{\omega}_f(t)}{\omega_h(t)} \approx \frac{\omega^*_f}{\omega^*_h} \tag{8}$$

To ensure that the compressor speed constraint in Eq. (7) is satisfied, $\hat{\omega}_f(t)$ is calculated as follows:

$$\hat{\omega}_f(t) = \begin{cases} \dfrac{\omega^*_f}{\omega^*_h} \cdot \omega_h(t) & \text{if } \dfrac{\omega^*_f}{\omega^*_h} \leq 1 \\ \omega_h(t) & \text{otherwise} \end{cases} \tag{9}$$

The application of a step change in $\hat{\omega}_f(t)$ causes a transient behavior in the system. Thus to ensure a smooth transition between set points, the speed set point for faulty chiller, $\omega^{sp}_f(t)$ should be gradually changed. A first order low pass filter is used to dampen the transient behavior, whose transfer

function is given by:

$$LP(s) = \frac{1}{\tau s + 1} \tag{10}$$

where $\tau = 300$ seconds. Finally, as mentioned earlier, the compressor speed $\omega_f(t)$ cannot be changed directly, since it is updated by the local controller which is not accessible. Thus, as an intermediate step we add a PI controller which determines the chilled water supply temperature set point of the faulty chiller $T^{sp}_{chws,f}(t)$ by monitoring the compressor speed sensor $\omega_f(t)$ in order to track the desired compressor speed $\omega^{sp}_f(t)$. The transfer function of this controller is:

$$G_f(s) = K_f \left(1 + \frac{1}{T_f s}\right) \tag{11}$$

where $K_f = -10$ and $T_f = 1$ second are the proportional gain and integral time, respectively.

V. RESULTS AND DISCUSSION

The results of the proposed supervisory control strategy are presented in this section. Inputs of weather and cooling load data for summer 2014 are used for generating the test data. The FDD module classifies each chiller as healthy, cautionary or critical. Based on the predicted fouling class, the supervisory controller switches to the resilient controller for the faulty chiller to mitigate the effects of fouling.

TABLE 6. Confusion matrices for classifier trained on summer 2013 using 4D feature space and tested on summer 2014.

		June'14 Classifier Output			July'14 Classifier Output		
		H	Ca	Cr	H	Ca	Cr
Actual Classes	H	240	15	0	250	5	0
	Ca	16	492	2	7	503	0
	Cr	0	9	310	0	0	319

		August'14 Classifier Output			Overall Classifier Output		
		H	Ca	Cr	H	Ca	Cr
Actual Classes	H	251	4	0	741	24	0
	Ca	14	496	0	37	1491	2
	Cr	0	1	318	0	10	947

A. FAULT DETECTION AND DIAGNOSIS

As discussed in Section IV-A1, different k-NN classification models are trained using the feature spaces consisting of different numbers of optimal sensors and T_{wb}, obtained from the data of months June-Aug'13. These feature spaces are then used for generating decisions for the test data from the months of June-Aug'14. It was observed that the feature space with four sensors provides the best classification accuracy. Table 6 shows the confusion matrices for the test data using the selected 4-D feature space. The numbers in the confusion matrices sum to the total number of test data blocks which is $\sim$ 1084 for each month.

TABLE 7. FDD performance for different months.

Testing Months	No. of Features	CCR (%)	FAR (%)
June'14	2	60.15	78.04
	3	95.11	6.27
	4	96.13	5.88
	5	95.94	6.27
July'14	2	64.39	87.84
	3	98.25	1.57
	4	98.89	1.96
	5	98.89	1.96
Aug'14	2	61.07	94.12
	3	97.23	1.57
	4	98.25	1.57
	5	98.25	1.57
Overall	2	61.90	86.54
	3	96.83	3.14
	4	97.76	3.14
	5	97.69	3.27

It is clear from Table 7 that the FDD scheme performs fouling classification with an accuracy of $\sim$ 97%. The confusion matrices in Table 6 show that the missed detection rate is minimized by the proposed scheme, thus providing good diagnosis. Importantly, any missed detections that do occur are between adjacent classes, e.g., a chiller in critical condition is never misclassified as healthy. The approach also has a low false alarm rate of about $\sim$ 3%, which is essential for a reliable FDD system. The robustness of the approach can be seen from the use of training and testing data from two different years. The classifier trained using data from the year 2013 gives accurate predictions for the data from 2014.

B. SUPERVISORY CONTROLLER

The performance of supervisory controller (SC) was tested for four different fouling levels, 25%, 40%, 55%, and 70%, over the months of June, July, and August of 2014 and compared against a chiller plant with no supervisory control ($NoSC$). Fig. 10 visualizes the results for a few snapshots of data taken during the first three days of July 2014 for 40% (Fig. 10(a)) and 70% (Fig. 10(b)) fouling.

First, the plot in the first column and the top row of each of the Figs. 10(a) and 10(b) shows the power savings which is the difference in power when the supervisory controller is not used with the one when it is used. As seen in these plots, the power savings are realized in almost all instances by up to about 20 kW. The corresponding plots below the power savings plots show that the supervisory controller also reliably tracks $T^{d}_{chws,p}$ in all instances of fouling. It is also noted that if the supervisory controller is not used for critical fouling cases of 70%, then the chiller plant does not meet the performance; however with the supervisory controller

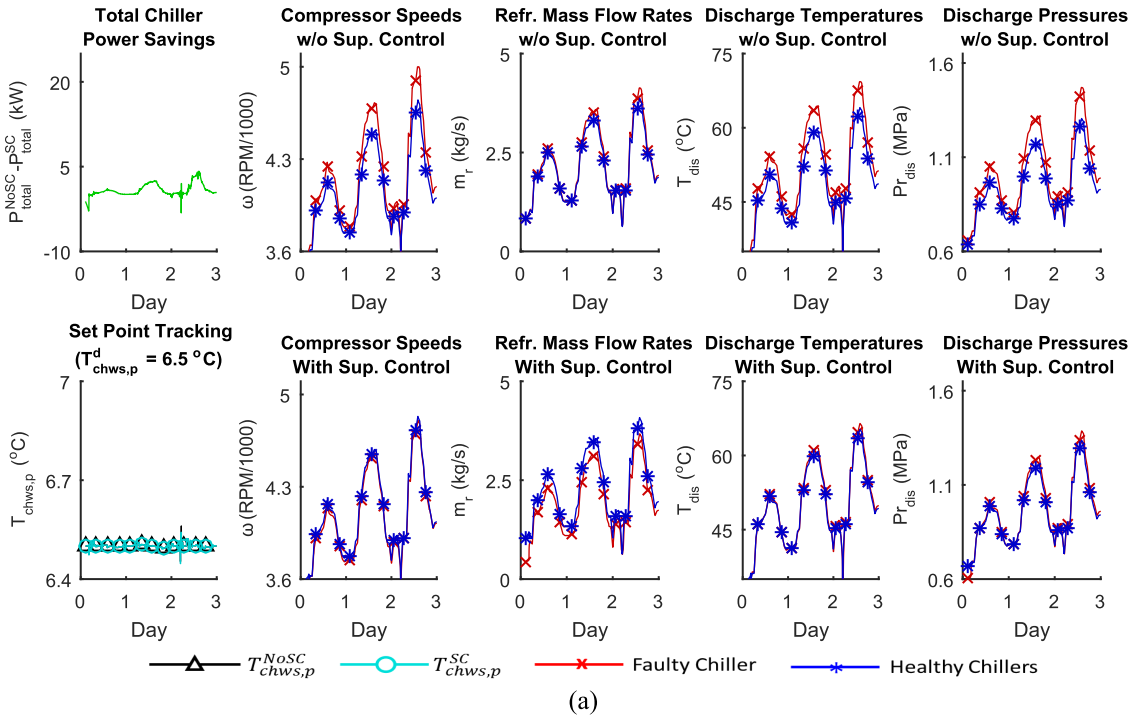

(a)

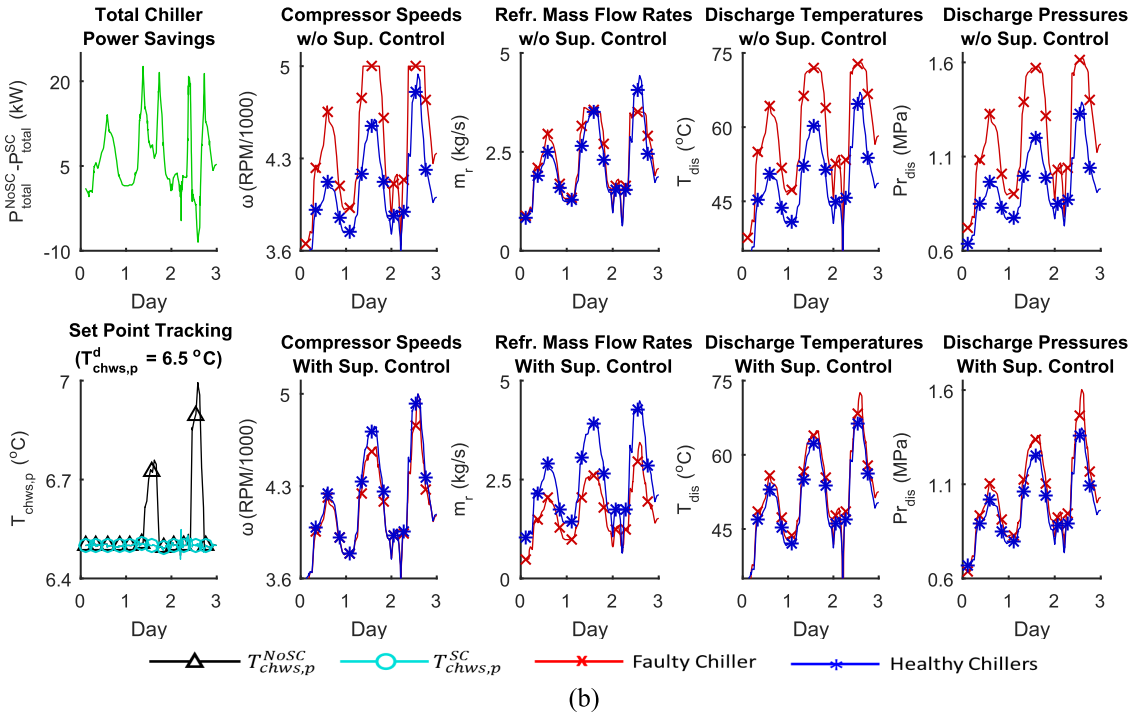

(b)

FIGURE 10. Supervisory control (SC) results compared with no supervisory control (NoSC) for the first three days of July 2014: (a) Results for the cautionary class (40% fouling) (b) Results for the critical class (70% fouling).

enabled, it does. Also, it is clear that tracking is smooth since there are no noticeable abrupt transient behaviors. To the right of these plots, in the second column, are the plots of compressor speeds ω_f and ω_h, with and without the supervisory control, respectively. As seen, ω_f is higher when no supervisory control is used. Also, when supervisory control is used, ω_f decreased by up to 500 RPM as the fouling level increases. In all cases, there is only a mild increase in ω_h

TABLE 8. Results of supervisory control when compared with no supervisory control during the summer months of 2014.

	25% Cautionary				40% Cautionary				55% Cautionary				70% Critical			
	June	July	Aug.	All	June	July	Aug.	All	June	July	Aug.	All	June	July	Aug.	All
RMSE $T_{chws,p}$ (°C)	2.8E-3	3.3E-3	2.5E-3	2.9E-3	2.9E-3	3.4E-3	2.6E-3	3.0E-3	2.9E-3	3.4E-3	2.7E-3	3.0E-3	3.3E-3	4.0E-3	3.5E-3	3.5E-3
ΔE_{total} **(kWh)**	12.6	10.1	-43.0	-20.3	157.9	329.9	112.0	599.8	562.6	1203.4	573.8	2339.8	1926.1	3491.3	2167.7	7585.1
Avg ΔP_{total} (%)	-0.24	0.04	-0.03	-0.08	0.01	0.33	0.17	0.17	0.65	1.11	0.78	0.85	2.66	3.05	2.66	2.79
Max ΔP_{total} (%)	5.13	1.41	1.44	5.14	5.63	1.64	2.08	5.63	5.85	2.74	3.13	5.85	7.05	6.62	7.26	7.26
Avg $\Delta\omega_f$ (%)	1.18	1.35	1.14	1.23	1.80	2.34	1.91	2.02	2.91	3.95	3.27	3.38	5.35	6.96	6.71	6.34
Max $\Delta\omega_f$ (%)	3.20	2.40	2.58	3.20	4.34	4.42	3.96	4.42	7.19	7.43	6.95	7.46	13.73	12.91	14.31	14.31
Avg $\Delta\omega_h$ (%)	-0.53	-0.64	-0.55	-0.58	-0.77	-1.04	-0.86	-0.89	-1.14	-1.60	-1.34	-1.36	-1.78	-2.49	-2.35	-2.21
Max $\Delta\omega_h$ (%)	-1.71	-1.54	-1.25	-1.71	-1.98	-1.92	-1.79	-1.98	-2.85	-2.91	-2.80	-2.91	-4.70	-4.30	-5.00	-5.00
Avg $\Delta T_{dis,f}$ (%)	3.51	2.26	2.40	2.72	4.90	3.81	3.89	4.20	7.37	6.31	6.44	6.71	12.14	11.01	12.90	12.02
Max $\Delta T_{dis,f}$ (%)	21.67	10.18	7.01	21.67	33.50	11.84	8.26	33.50	34.44	14.54	10.34	34.44	37.18	19.35	38.57	38.57
Avg $\Delta T_{dis,h}$ (%)	-1.35	-1.07	-1.14	-1.19	-1.84	-1.70	-1.74	-1.76	-2.58	-2.58	-2.65	-2.60	-3.81	-3.93	-4.56	-4.10
Max $\Delta T_{dis,h}$ (%)	-6.56	-5.32	-2.96	-6.56	-6.78	-5.57	-3.37	-6.78	-7.25	-5.86	-3.96	-7.25	-7.69	-6.61	-8.55	-8.55
Avg $\Delta Pr_{dis,f}$ (%)	2.52	2.40	2.30	2.41	3.82	4.18	3.86	3.96	6.20	7.22	6.71	6.71	11.40	13.23	13.94	12.86
Max $\Delta Pr_{dis,f}$ (%)	9.39	8.33	4.97	9.39	10.58	9.44	6.69	10.58	12.67	11.34	11.49	12.67	22.84	21.39	24.30	24.30
Avg $\Delta Pr_{dis,h}$ (%)	-1.19	-1.11	-1.07	-1.12	-1.64	-1.77	-1.64	-1.68	-2.34	-2.70	-2.53	-2.52	-3.52	-4.10	-4.39	-4.00
Max $\Delta Prdis,h$ (%)	-4.72	-4.11	-2.39	-4.72	-4.88	-4.30	-2.89	-4.88	-5.22	-4.52	-4.39	-5.22	-7.26	-6.57	-7.89	-7.89
Avg $\Delta\dot{m}_{r,f}$ (%)	11.49	7.12	8.16	8.92	15.08	11.40	12.42	12.97	20.66	17.69	18.97	19.11	29.99	27.86	32.82	30.22
Max $\Delta\dot{m}_{r,f}$ (%)	56.81	49.40	33.97	56.81	57.51	50.56	36.14	57.51	57.93	50.79	39.67	57.93	58.77	53.29	62.98	62.98
Avg $\Delta\dot{m}_{r,h}$ (%)	-5.84	-3.57	-4.10	-4.50	-7.62	-5.65	-6.20	-6.49	-10.37	-8.60	-9.42	-9.46	-14.86	-13.07	-16.17	-14.70
Max $\Delta\dot{m}_{r,h}$ (%)	-29.71	-25.85	-17.43	-29.71	-30.20	-26.51	-18.80	-30.20	-30.39	-26.59	-20.30	-30.39	-30.82	-27.77	-33.38	-33.38

by up to 100 RPM, showing that the healthy chillers are not significantly overdriven. This reduction in the faulty chiller compressor speed, as expected, reduces the mass flow rate of the refrigerant. This reduction in flow, in turn, reduces the faulty chiller discharge temperature and pressure at the condenser inlet, which signifies a reduction of stress on the chiller and its components. At the same time, there are only modest increases in the mass flow rate, discharge temperature, and discharge temperature of the healthy chillers, reinforcing the notion that these chillers do not work much harder due to load redistribution from the faulty chiller. Thus, the supervisory controller clearly mitigates the adverse effects of condenser fouling until maintenance can be performed.

Table 8 summarizes the results over the summer months of 2014. The root mean squared error (RMSE) of the performance variable $T_{chws,p}$ was calculated as follows:

$$\textbf{RMSE } T_{chws,p} = \sqrt{\frac{1}{\tau}\int_0^\tau \left(T_{chws,p}(t) - T^d_{chws,p}(t)\right)^2 dt} \ ^\circ\text{C}$$

where τ is the total time during the months June, July, and August of 2014. The RMSE was consistently low with a maximum observed value of 4.0E-3 °C during extreme fouling condition. This shows that the supervisory controller reliably meets the required cooling load performance. The effects of supervisory control (SC) action are shown on different system parameters in comparison to no supervisory control (NoSC). For example, the average power reduction is defined as:

$$\textbf{Avg } \Delta P_{total} = \frac{1}{\tau}\int_0^\tau \left(\frac{P^{NoSC}_{total}(t) - P^{SC}_{total}(t)}{P^{NoSC}_{total}(t)}\right) dt \times 100\%$$

and the maximum power reduction is defined as:

$$\textbf{Max } \Delta P_{total} = \max_t \frac{P^{NoSC}_{total}(t) - P^{SC}_{total}(t)}{P^{NoSC}_{total}(t)} \times 100\%$$

Except for low fouling levels, where its effects on the chiller plant are small, the power consumption always decreases with the supervisory controller active by up to 3.05% on average and 7.26% maximum, yielding up to 7585 kWh of energy savings, where the energy savings are defined as:

$$\Delta E_{total} = \frac{\int_0^\tau P^{NoSC}_{total}(t) - P^{SC}_{total}(t)dt}{3.6 \times 10^6} \text{ kWh}$$

The average and maximum changes for the healthy and faulty chiller speeds, discharge temperatures, discharge pressures and refrigerant mass flow rates, are calculated in the same manner as for ΔP_{total}. Overall, the faulty chiller sees significant speed reduction between 1.23% to 6.34% on average for different fouling levels. Similarly, the maximum speed reduction ranged from 3.20% to 14.31% depending on the fouling severity. On the other hand, the speed increases for the healthy chillers were minimal ranging from 0.58% and 2.21% on average. The discharge temperature $T_{dis,f}$, discharge pressures $Pr_{dis,f}$, and refrigerant mass flow rate $\dot{m}_{r,f}$ in the faulty chiller show maximum reductions of up to 38.57%, 24.30%, and 62.98%, respectively, thus showing a significant decrease in the stress on different components of the chiller. The healthy chillers see comparatively much smaller increases in these parameters.

Overall, these results demonstrate that the supervisory controller is able to meet the required performance for the

customer under condenser fouling while providing resilience. Notably, the main features of this supervisory controller for the end user include:

- cost savings through reduced energy consumption,
- increased product lifespan through faulty chiller load reduction,
- chiller plant performance guarantees through load redistribution to health chillers, and
- conditioned-based maintenance to ensure fouling is treated only when needed.

These features can collectively provide considerable cost savings to end user over the life cycle of the chiller plant. The proposed supervisory control strategy can be implemented on a real chiller plant by integrating the supervisory control framework with the Plant System Manager (PSM).

VI. CONCLUSIONS AND FUTURE WORK

This paper proposed a novel model-based supervisory control framework that enables resilient operation of chiller plants in the presence of condenser fouling. The supervisory control framework consists of an optimal sensor selection-based fault detection and diagnosis scheme and a resilient control strategy that effectively mitigates the effects of condenser fouling by bringing the system parameters back to normalcy, while meeting the cooling load demand. The methodology is validated on a high-fidelity chiller plant model where it is shown to meet all of its listed goals. The FDD approach shows high classification accuracy with low missed detection and false alarm rates, while the supervisory control results demonstrate resilience, power savings, and cooling load performance guarantees, for different fouling severities and for operation during different months. Furthermore, these solutions are shown to be robust by extensive testing on a large and diverse data set and are computationally efficient due to the simplicity of their designs.

For future work, the methodology needs to be extended to provide a resilient control action against all the major faults in chillers and chiller plants. However, to design a control strategy to handle multiple faults, the fault detection and diagnosis strategy needs to be improved by incorporating system-level fault detection and isolation, which monitors the entire chiller plant and identifies exactly which component or subcomponent in a chiller plant is faulty. Other areas for improvement are updating the control to handle chiller start-up and shut-down times, chiller staging and asymmetric chiller configurations. Comparison of the obtained results with real experimental condenser fouling data if available or simulated sensor data with more uncertainty in terms of bias and noise values is another area of future work. Finally, improvements to the proposed algorithms that minimize the amount of required training data will increase the scalability of the supervisory controller when dealing with larger problems. The supervisory control framework presented here can be extended and applied to other complex interconnected systems with load sharing subsystems such as airplanes, power grids, smart buildings, etc. to achieve energy-efficient and reliable operation.

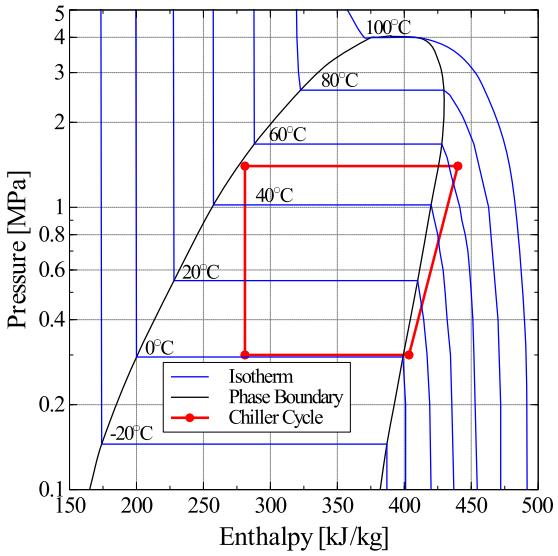

FIGURE 11. Thermodynamic cycle of the chiller model at nominal conditions.

APPENDIX
VALIDATION OF CHILLER PLANT MODEL

The high-fidelity chiller plant simulation model is implemented in the Modelica modeling language using component models from several commercial and open-source libraries. The models used in this work are a high-fidelity model of a water-cooled centrifugal chiller with local capacity control and a scalable framework model of a chiller plant, which uses the chiller model as a component. Local capacity control of the chiller adjusts its compressor speed to maintain a chilled water supply temperature setpoint, which is assigned at the plant level. The chiller plant testbed model includes component models representing the key components of a closed loop chilled water plant. The chiller components in the plant model are interchangeable, allowing for side-by-side comparison between the high-fidelity chiller model and existing alternatives.

Validation of the high fidelity chiller model was undertaken by first comparing its outputs to published standards for chillers using the selected refrigerant at nominal operating conditions, as enumerated in Table 9. With these values in agreement the chiller model is a realistic representation of an R134a refrigeration cycle. The thermodynamic cycle of the chiller model at nominal conditions is illustrated in Fig. 11.

Validation of the chiller plant model was performed by comparison of its outputs to operating data recorded from the chiller plant in the University of Connecticut Central Utilities Plant (UConn CUP) and corresponding weather data. Two plant model configurations were evaluated, one using the developed high-fidelity chiller model and the other using an existing validated empirical chiller model from the LBNL Buildings Library. Both model configurations were found to suitably represent the behavior of a real chiller plant for the

TABLE 9. High fidelity model nominal conditions.

Variable	Unit	Standard Value	Simulation Result
Condenser Inlet Pressure	[kPa]	1410	1400
Evaporator Outlet Pressure	[kPa]	300	301
Pressure Ratio		4.7 : 1	4.65 : 1
Condenser Outlet Temperature	[°C]	54	52
Evaporator Outlet Superheat	[°C]	5	5

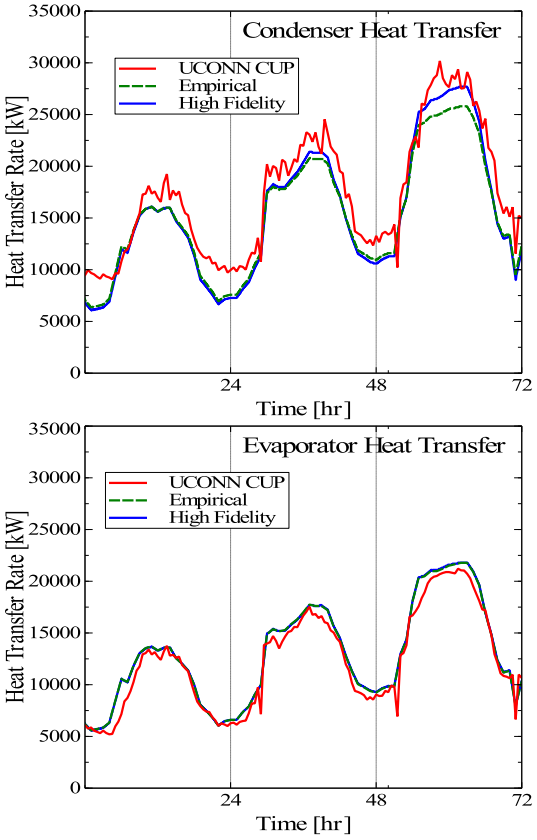

FIGURE 12. Comparison of the heat transfer rates on the condenser and evaporator sides of the chillers in the proposed model with real chiller plant and empirical models.

studied range of input conditions, confirming the validity of both the chiller and chiller plant models used in this work. Fig. 12 shows a comparison of heat transfer rates on the condenser and evaporator sides of the chillers in each of these models and the real chiller plant.

REFERENCES

[1] F. W. Payne and J. J. McGowan, *Energy Management and Control Systems Handbook*. Lilburn, GA, USA: Springer, 2012.
[2] L. Pérez-Lombard, J. Ortiz, and C. Pout, "A review on buildings energy consumption information," *Energy Buildings*, vol. 40, no. 3, pp. 394–398, 2008.
[3] K. Choi, S. M. Namburu, M. S. Azam, J. Luo, K. R. Pattipati, and A. Patterson-Hine, "Fault diagnosis in HVAC chillers," *IEEE Instrum. Meas. Mag.*, vol. 8, no. 3, pp. 24–32, Aug. 2005.
[4] M. Comstock, J. Braun, and E. Groll, "The sensitivity of chiller performance to common faults," *HVACR Res.*, vol. 7, no. 3, pp. 263–279, 2001.
[5] X. Zhao, M. Yang, and H. Li, "A virtual condenser fouling sensor for chillers," *Energy Buildings*, vol. 52, pp. 68–76, Sep. 2012.
[6] J. Tomczyk, *Troubleshooting and Servicing Modern Air Conditioning and Refrigeration Systems*. Mt. Prospect, Il, USA: ESCO Press, 1995.
[7] J. Tomczyk. (2002). *A Look at Compressor Discharge Temperatures*. [Online]. Available: http://www.achrnews.com/articles/88734-a-look-at-compressor-discharge-temperatures#comments
[8] ThermaCom Ltd. (2000). *Compressor Longevity*. [Online]. Available: http://seedengr.com/CompressorLongevity.pdf
[9] S. Sridhar, A. Hahn, and M. Govindarasu, "Cyber attack-resilient control for smart grid," in *Proc. IEEE PES Innov. Smart Grid Technol. (ISGT)*, Jan. 2012, pp. 1–3.
[10] C. G. Rieger, D. I. Gertman, and M. A. McQueen, "Resilient control systems: Next generation design research," in *Proc. 2nd Conf. Human Syst. Interaction*, May 2009, pp. 632–636.
[11] D. L. Alderson and J. C. Doyle, "Contrasting views of complexity and their implications for network-centric infrastructures," *IEEE Trans. Syst., Man, Cybern. A, Syst., Humans*, vol. 40, no. 4, pp. 839–852, Jul. 2010.
[12] D. Wei and K. Ji, "Resilient industrial control system (RICS): Concepts, formulation, metrics, and insights," in *Proc. 3rd Int. Symp. Resilient Control Syst. (ISRCS)*, 2010, pp. 15–22.
[13] Z. Ma, S. Wang, X. Xu, and F. Xiao, "A supervisory control strategy for building cooling water systems for practical and real time applications," *Energy Convers. Manage.*, vol. 49, no. 8, pp. 2324–2336, 2008.
[14] Z. Ma and S. Wang, "Supervisory and optimal control of central chiller plants using simplified adaptive models and genetic algorithm," *Appl. Energy*, vol. 88, no. 1, pp. 198–211, 2011.
[15] X. Wei, A. Kusiak, M. Li, F. Tang, and Y. Zeng, "Multi-objective optimization of the HVAC (heating, ventilation, and air conditioning) system performance," *Energy*, vol. 83, pp. 294–306, Apr. 2015.
[16] S. Wang and Z. Ma, "Supervisory and optimal control of building HVAC systems: A review," *HVACR Res.*, vol. 14, no. 1, pp. 3–32, 2008.
[17] Y. Zeng, Z. Zhang, and A. Kusiak, "Predictive modeling and optimization of a multi-zone HVAC system with data mining and firefly algorithms," *Energy*, vol. 86, pp. 393–402, Jun. 2015.
[18] A. Kusiak and G. Xu, "Modeling and optimization of HVAC systems using a dynamic neural network," *Energy*, vol. 42, no. 1, pp. 241–250, 2012.
[19] S. Wang and Y. Chen, "Fault-tolerant control for outdoor ventilation air flow rate in buildings based on neural network," *Building Environ.*, vol. 37, no. 7, pp. 691–704, 2002.
[20] X. Jin and Z. Du, "Fault tolerant control of outdoor air and AHU supply air temperature in VAV air conditioning systems using PCA method," *Appl. Thermal Eng.*, vol. 26, no. 11, pp. 1226–1237, 2006.
[21] K. Ji, Y. Lu, L. Liao, Z. Song, and D. Wei, "Prognostics enabled resilient control for model-based building automation systems," in *Proc. 12th Conf. Int. Building Perform. Simulation Assoc.*, 2011, pp. 286–293.
[22] Z. Ma and S. Wang, "Online fault detection and robust control of condenser cooling water systems in building central chiller plants," *Energy Buildings*, vol. 43, no. 1, pp. 153–165, 2011.
[23] Z. Ma and S. Wang, "Fault-tolerant supervisory control of building condenser cooling water systems for energy efficiency," *HVACR Res.*, vol. 18, nos. 1–2, pp. 126–146, 2012.
[24] X.-F. Liu and A. Dexter, "Fault-tolerant supervisory control of VAV air-conditioning systems," *Energy Buildings*, vol. 33, no. 4, pp. 379–389, 2001.
[25] S. Katipamula and M. R. Brambley, "Review article: Methods for fault detection, diagnostics, and prognostics for building systems—A review, part I," *HVACR Res.*, vol. 11, no. 1, pp. 169–187, 2005.
[26] Y. Yu, D. Woradechjumroen, and D. Yu, "A review of fault detection and diagnosis methodologies on air-handling units," *Energy Buildings*, vol. 82, pp. 550–562, Oct. 2014.
[27] Y. Zhang and J. Jiang, "Bibliographical review on reconfigurable fault-tolerant control systems," *Annu. Rev. Control*, vol. 32, no. 2, pp. 229–252, 2008.
[28] J. Cui and S. Wang, "A model-based online fault detection and diagnosis strategy for centrifugal chiller systems," *Int. J. Thermal Sci.*, vol. 44, no. 10, pp. 986–999, 2005.

[29] T. A. Reddy, "Development and evaluation of a simple model-based automated fault detection and diagnosis (FDD) method suitable for process faults of large chillers," *ASHRAE Trans.*, vol. 113, no. 2, pp. 27–39, 2007.
[30] M. Bonvini, M. D. Sohn, J. Granderson, M. Wetter, and M. A. Piette, "Robust on-line fault detection diagnosis for HVAC components based on nonlinear state estimation techniques," *Appl. Energy*, vol. 124, pp. 156–166, Jul. 2014.
[31] Q. Zhou, S. Wang, and Z. Ma, "A model-based fault detection and diagnosis strategy for HVAC systems," *Int. J. Energy Res.*, vol. 33, no. 10, pp. 903–918, 2009.
[32] S. Wang and J. Cui, "A robust fault detection and diagnosis strategy for centrifugal chillers," *HVACR Res.*, vol. 12, no. 3, pp. 407–428, 2006.
[33] Y. Chen, X. Hao, G. Zhang, and S. Wang, "Flow meter fault isolation in building central chilling systems using wavelet analysis," *Energy Convers. Manage.*, vol. 47, no. 13, pp. 1700–1710, 2006.
[34] W.-Y. Lee, J. M. House, and N.-H. Kyong, "Subsystem level fault diagnosis of a building's air-handling unit using general regression neural networks," *Appl. Energy*, vol. 77, no. 2, pp. 153–170, 2004.
[35] R. Hackner, W. Beckman, and J. Mitchell, "System dynamics and energy use," *ASHRAE J.*, vol. 27, no. 6, Jun. 1985.
[36] J. Braun, "Methodologies for the design and control of central cooling plants," Ph.D. dissertation, Dept. Mech. Eng., Univ. Wisconsin-Madison, Madison, WI, USA, 1988.
[37] J. U. R. Khan and S. M. Zubair, "Thermodynamic optimization of finite time vapor compression refrigeration systems," *Energy Convers. Manage.*, vol. 42, no. 12, pp. 1457–1475, 2001.
[38] *Basic Concepts Manual—Essential Information You Need about Running EnergyPlus*, US Dept. Energy Nat. Renewable Energy Lab. (NREL), Golden, Colorado, 2013.
[39] *DOE-2 Reference Manual*, Los Alamos Sci. Lab., Los Alamos, NM, USA, 1980.
[40] *Trnsys 17 User Guide*, Univ. Wisconsin Madison, Madison, WI, USA, 2009.
[41] Modelica Association. (2014). *The Modelica Language Specification Version 3.3 Revision 1*. [Online]. Available: http://www.modelica.org/
[42] *Dymola User's Manual*, Dynasim AB, Vélizy-Villacoublay, France, 2004.
[43] M. Wetter, "A Modelica-based model library for building energy and control systems," Lawrence Berkeley Nat. Lab., Berkeley, CA, USA, Tech. Rep. LBNL-2739E, 2010.
[44] S. Quoilin, A. Desideri, J. Wronski, I. Bell, and V. Lemort, "Thermocycle: A modelica library for the simulation of thermodynamic systems," in *Proc. 10th Int. Modelica Conf.*, 2014, pp. 683–692.
[45] *Dymola User's Manual*, Dynasim AB, Vélizy-Villacoublay, France, 2014.
[46] (2015). *National Weather Service*. [Online]. Available: http://www.weather.gov
[47] B. P. Baillie and G. M. Bollas, "Development, validation, and assessment of a high fidelity chilled water plant model," *Appl. Thermal Eng.*, vol. 111, pp. 477–488, Jan. 2017.
[48] X. Zhao, M. Yang, and H. Li, "A virtual condenser fouling sensor for chillers," *Energy Buildings*, vol. 52, pp. 68–76, Sep. 2012. [Online]. Available: http://www.sciencedirect.com/science/article/pii/S0378778812002733
[49] T. Cover and P. Hart, "Nearest neighbor pattern classification," *IEEE Trans. Inf. Theory*, vol. 13, no. 1, pp. 21–27, Jan. 1967.
[50] D. L. Donoho and J. M. Johnstone, "Ideal spatial adaptation by wavelet shrinkage," *Biometrika*, vol. 81, no. 3, pp. 425–455, 1994.
[51] D. L. Donoho, "De-noising by soft-thresholding," *IEEE Trans. Inf. Theory*, vol. 41, no. 3, pp. 613–627, May 1995.
[52] R. Kohavi and G. H. John, "Wrappers for feature subset selection," *Artif. Intell.*, vol. 97, nos. 1–2, pp. 273–324, 1997.
[53] H. Peng, F. Long, and C. Ding, "Feature selection based on mutual information criteria of max-dependency, max-relevance, and min-redundancy," *IEEE Trans. Pattern Anal. Mach. Intell.*, vol. 27, no. 8, pp. 1226–1238, Aug. 2005.
[54] R. Kohavi *et al.*, "A study of cross-validation and bootstrap for accuracy estimation and model selection," in *Proc. IJCAI*, vol. 14. 1995, pp. 1137–1145.
[55] D. Arthur and S. Vassilvitskii, "K-means++: The advantages of careful seeding," in *Proc. 18th Annu. ACM-SIAM Symp. Discrete Algorithms*, Philadelphia, PA, USA, 2007, pp. 1027–1035.

KHUSHBOO MITTAL received the B.E. degree in electronics and communication engineering from IIT Roorkee, India, in 2011, and the M.S. degree in electrical engineering from the École Polytechnique Fédérale de Lausanne, Switzerland, in 2013. She is currently pursuing the Ph.D. degree with the Department of Electrical and Computer Engineering, University of Connecticut, Storrs, CT, USA. Her current research interests include data analysis in complex network systems, fault diagnosis and prognosis, machine learning, sensor/feature selection, and information fusion.

JAMES P. WILSON received the B.S.E. degree in electrical engineering from the University of Connecticut, Storrs, CT, USA, in 2014, where he is currently pursuing the Ph.D. degree with the Department of Electrical and Computer Engineering. His current research interests include data analysis, machine learning, fault diagnosis and prognosis, and supervisory control in complex interconnected systems in the presence of faults and degradations.

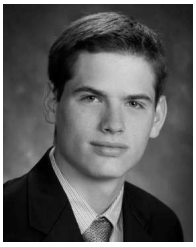

BRIAN P. BAILLIE received the B.S.E. degree in chemical engineering from the University of Connecticut, Storrs, CT, USA, in 2014, where he is currently pursuing the Ph.D. degree with the Department of Chemical and Biomolecular Engineering. His research interests include the modeling of complex thermofluid systems, heuristic-informed generation of reduced models, and optimal experimental design for model selection.

SHALABH GUPTA (M'07) received the B.E. degree in mechanical engineering from IIT Roorkee, India, in 2001, and the M.S. degree in mechanical engineering, the M.S. degree in electrical engineering, and the Ph.D. degree in mechanical engineering from Pennsylvania State University, University Park, PA, USA, in 2004, 2005, and 2006, respectively. He is currently an Assistant Professor with the Department of Electrical and Computer Engineering, University of Connecticut. His current research interests include distributed autonomy, cyber-physical systems, robotics, network intelligence, data analytics, information fusion, and fault diagnosis in complex systems. He is a member of the American Society of Mechanical Engineers.

GEORGE M. BOLLAS received the B.E. and Ph.D. degrees from the Aristotle University of Thessaloniki, Greece. He was a Post-Doctoral Research Associate with the Chemical Engineering Department, Massachusetts Institute of Technology. He is currently an Associate Professor with the Department of Chemical and Biomolecular Engineering, University of Connecticut, a Process Design Expert and Winner of the prestigious NSF CAREER Award and the ACS PRF DNI Award. He is the Director of the United Technologies Corporation Institute for Advanced Systems Engineering with the University of Connecticut. His laboratory pursues a balanced approach to experimentation guided by robust modeling and simulation of chemical processes, including experimental design, process scaling, and control.

PETER B. LUH (S'77–M'80–SM'91–F'95–LF'16) received the B.S. degree from National Taiwan University, Taipei, Taiwan, the M.S. degree from the Massachusetts Institute of Technology, Cambridge, MA, USA, and the Ph.D. degree from Harvard University, Cambridge. He has been with the University of Connecticut, Storrs, CT, USA, since 1980, and is the SNET Professor of Communications and Information Technologies. His current research interests include smart and green buildings, intelligent manufacturing, and smart grid. He is a member and the Elected Chair (2018–2019) of the IEEE TAB Periodicals Committee. He was the Vice President of publication activities for the IEEE Robotics and Automation Society, an Editor-in-Chief of the IEEE TRANSACTIONS ON ROBOTICS AND AUTOMATION, and the Founding Editor-in-Chief of the IEEE TRANSACTIONS ON AUTOMATION SCIENCE AND ENGINEERING.